

Pulsed laser deposition film of a donor–acceptor–donor polymer as possible active layer in devices

K. Ranjith · S. K. Swathi · Prajwal Kumar ·
Praveen C. Ramamurthy

Received: 12 August 2010/Accepted: 9 November 2010/Published online: 30 November 2010
© Springer Science+Business Media, LLC 2010

Abstract A molecule having a ketone group between two thiophene groups was synthesized. Presence of alternating electron donating and accepting moieties gives this material a donor–acceptor–donor (DAD) architecture. PolyDAD was synthesized from DAD monomer by oxidative polymerization. Device quality films of polyDAD were fabricated using pulsed laser deposition technique. X-ray photoelectron spectroscopy (XPS) and fourier transform infrared spectra (FTIR) data of both as synthesized and film indicate the material does not degrade during ablation. Optical band gap was determined to be about 1.45 eV. Four orders of magnitude increase in conductivity was observed from as synthesized to pulsed laser deposition (PLD) fabricated film of polyDAD. Annealing of polyDAD films increase conductivity, indicating better ordering of the molecules upon heating. Rectifying devices were fabricated from polyDAD, and preliminary results are discussed.

Introduction

Conducting polymers and their derivatives are widely used in electronic applications because of their tailorabile electronic properties [1]. Organic electronics development raises an ever increasing scientific interest due to their low cost and mechanical flexibility [2–4]. Most of the electro active

polymers show relatively facile synthetic access, environmental stability, and solution processability. Absorption range of these conjugated polymers can be modified by substitution of different moieties in the repeating unit [5, 6]. Substitution of electron rich and poor moieties in the repeating units results in the formation of donor–acceptor structures [7].

Bulk heterojunction structures have been successfully employed in case of organic solar cells [8–10]. However, there are few issues associated with the efficiency of organic solar cells, such as light absorption, exciton formation, exciton dissociation, and charge transportation [11–13]. Donor–acceptor–donor (DAD) structured materials could increase the efficiency of organic devices by enhancing exciton dissociation, light absorption, and charge transportation. In cyclopentadithiophene, where thiophene acts as an electron donating group, addition of a molecule having a ketone group between two thiophene groups can act as a DAD structure [14–16]. In this study, the synthesis of DAD structured material in which, thiophene moiety acts as an electron donating group and ketone as an electron accepting group is described [17]. Central acceptor ring locks the two external rings in a planar conformation [18].

Furthermore, morphology of the film plays an important role in defining efficiency of solar cells. Device performance could be enhanced by controlling the morphology of the film [19–21]. Device quality films of many conducting polymers with excellent electrical properties can not be fabricated, because neither they are soluble in most organic solvents nor it can melt [22]. To deposit extremely pure material films, pulsed laser deposition (PLD) is an ideal technique. Thin film growth by PLD method involves evaporation of a solid target in a high vacuum chamber by means of short and high-energy laser pulses. A pulsed laser

Electronic supplementary material The online version of this article (doi:[10.1007/s10853-010-5065-4](https://doi.org/10.1007/s10853-010-5065-4)) contains supplementary material, which is available to authorized users.

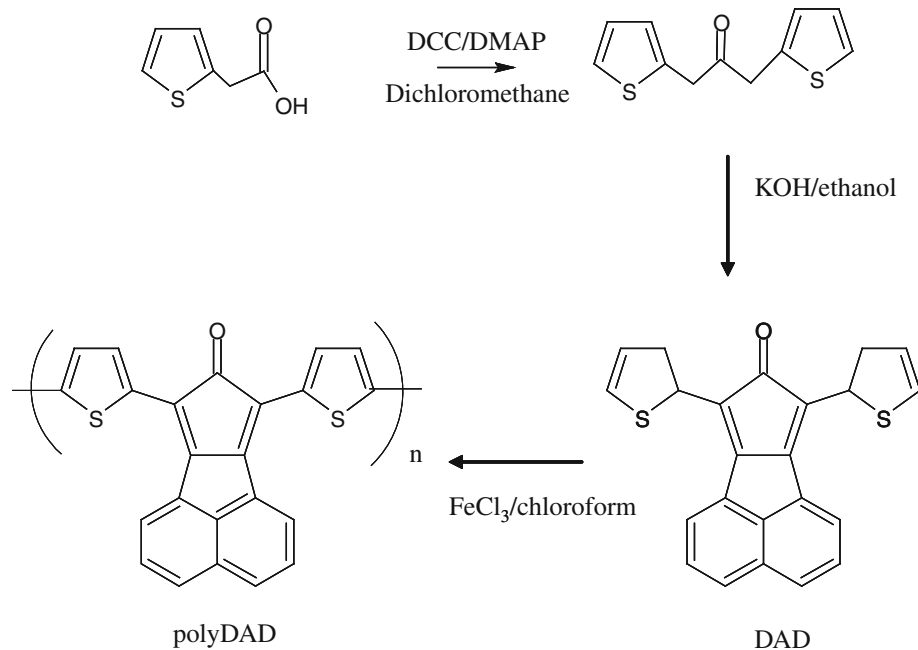
K. Ranjith · S. K. Swathi · P. Kumar · P. C. Ramamurthy (✉)
Department of Materials Engineering, Indian Institute
of Science, Bangalore 560012, India
e-mail: praveen@materials.iisc.ernet.in

beam vaporizes the surface of the target, and the vapor condenses on a substrate. It is possible to obtain the desired film stoichiometry for multi-element materials using PLD. In some materials, PLD produces fine particulates chunks of target material ranging in size from microns down to submicron dimensions [23, 24]. There is a lot of interest in laser ablation technique because films can be fabricated even from insoluble and/or unprocessable polymers from any other conventional method. Laser ablation methods for various polymers have been evaluated in the past [20, 25]. In this study, device quality film of polymer with DAD structured repeating unit, which is insoluble, is fabricated by PLD.

Experimental procedure

DAD structured polymer was synthesized by chemical oxidative polymerization of 7,9-di (thiophen-2-yl)-8H-cyclopenta[a]acenaphthylen-8-one in the presence of ferric chloride. Intermediate compound di (thiophene-2-yl) propane-2-one was synthesized by self condensation of thiophene acetic acid using dicyclohexylcarbodiimide and dimethylaminopyridine. Monomeric unit, 7,9-di (thiophen-2-yl)-8H-cyclopenta[a]acenaphthylen-8-one was obtained as a dark green solid by double Knoevenagel condensation with acenaphthenequinone and di(thiophene-2-yl) propane-2-one. Chemical oxidative polymerization of the resulting compound in the presence of ferric chloride yields poly7,9-di (thiophen-2-yl)-8H-cyclopenta[a]acenaphthylen-8-one as a black insoluble solid (Fig. 1).

Fig. 1 Synthesis scheme for monomer (DAD) and polymer (polyDAD)



Materials

2-Thiophene acetic acid, dicyclohexylcarbodiimide (DCC), dimethylaminopyridine (DMAP), and acenaphthenequinone were purchased from Sigma-Aldrich and used without further purification. Solvents dichloromethane, ethanol, tetrahydrofuran (THF), and chloroform obtained from local supplier were distilled before use. Silica gel of 100–200 and 230–400 meshes were used for column chromatography.

Synthesis of di (thiophen-2-yl) propan-2-one

2-Thiophene acetic acid (5 g, 0.0352 mol) in anhydrous dichloromethane (30 mL) was added drop wise to a stirred solution of DCC (7.6 g, 0.0368 mol) and DMAP (1.23 g, 0.01 mol) in anhydrous dichloromethane (70 mL) at 0 °C. Reaction was carried out for 12 h at room temperature in an inert atmosphere. Byproduct urea was removed by filtration, and the filtrate was purified by column chromatography with petroleum ether and ethyl acetate as eluent (1–5% PE/EA). Yield = 62.2%. ^1H NMR spectrum (CDCl_3 , δ in ppm) 7.21–7.23(2H, d), 6.95–6.99(2H, dd), 6.85–6.90(2H, d), 3.99(4H, s); HRMS (ESI, m/z): ($M + \text{Na}$) calculated for $\text{C}_{11}\text{H}_{10}\text{OS}_2$, 245.3165; found, 245.0071 (see supporting information Figs. 1 and 2).

Synthesis of 7,9-di (thiophen-2-yl)-8H-cyclopenta[a]acenaphthylen-8-one (DAD)

Di (thiophen-2-yl) propan-2-one (1.5 g, 6.75 mmol) and 1.23 g of acenaphthenequinone (1.23 g, 6.75 mmol) in

75 mL of ethanol (75 mL) are refluxed in a round bottom flask. Two pellets of potassium hydroxide dissolved in ethanol (3 mL) were added drop wise when the reaction mixture becomes homogenous. When the solution turned to dark green color, mixture was quenched into an ice bath. Resulting product was filtered, washed with cold ethanol and hot hexane, respectively. Product was dried under vacuum. Yield = 62%. ^1H NMR spectrum (CDCl_3 , δ in ppm): 8.413–8.431(2H, d), 7.924–7.935(2H, dd), 7.879–7.899(2H, d), 7.655–7.694(2H, t), 7.494–7.509(2H, dd) 7.216–7.259(2H). HRMS (ESI, m/z): ($M + \text{Na}$) calculated for $\text{C}_{23}\text{H}_{12}\text{OS}_2$, 391.4608; found 391.0227 (see supporting information Figs. 3 and 4).

Synthesis of poly7,9-di (thiophen-2-yl)-8H-cyclopenta[a]acenaphthylen-8-one (polyDAD)

Poly7,9-di (thiophen-2-yl)-8H-cyclopenta[a]acenaphthylen-8-one was synthesized by chemical oxidative polymerization of 7,9-di (thiophen-2-yl)-8H-cyclopenta[a]acenaphthylen-8-one using ferric chloride. FeCl_3 (2.82 g) was added to a stirred solution of 7,9-di (thiophen-2-yl)-8H-cyclopenta[a]acenaphthylen-8-one (1 g) in anhydrous chloroform (40 mL). Reaction was carried out under nitrogen atmosphere for 12 h. Resulting mixture was filtered and washed with aqueous ammonium hydroxide to precipitate the ferric chloride as ferric hydroxide. Residual solid was further heated in THF (50 mL) and washed with copious amount of methanol, chloroform, and THF to remove the ferric hydroxide formed. Remaining iron content (determined by ammonium thiocyanate test) was removed by washing with hydrochloric acid (2 M) and de-ionized water, respectively. Product was dried under vacuum. Yield = 60%. FTIR (KBr pellet cm^{-1}): 1701(C=O), 1582 (aromatic 1,2,3 trisubstituted ring), 1476 (C–H asymmetrical deformation), 1030 (aromatic 1,2,3 trisubstituted C–H bend), 1140 (C–H bend), 763 (aromatic 1,2,3 trisubstituted C–H def), 3052 (aromatic 1,2,3 trisubstituted C–H stretching) (see supporting information Fig. 5).

Film and device fabrication

Pellets of DAD and polyDAD with 1-cm diameter and 5-mm thickness were used for fabricating films using PLD technique. Pellets were fabricated using desktop press, with applied load of 10 ton. Care is taken to keep the pellet thickness above 3 mm to safeguard the integrity of the target during ablation. Wavelength and energy used for the deposition process were 1064 nm and 50 mJ, respectively under a vacuum of 6×10^{-6} Torr. Target and the substrate separated by 5 cm were rotated at 60 rpm to obtain a uniform deposition. Films were deposited on different substrates, i.e., silicon, glass, and ITO in a single ablation to minimize the batch to batch process variation that might

occur. The films deposited on ITO were used to fabricate a rectifying device. Films on glass and silicon wafer were used to characterize material property. A thin film of polyDAD (<50 nm) was deposited on the sodium chloride (NaCl) crystal for transmission electron microscopy (TEM) analysis. The NaCl crystal was dissolved in de-ionized water to obtain free standing film. As obtained free standing of polyDAD film was lifted on to 300 mesh carbon-coated copper grid for TEM analysis. In the case of DAD, the film was scraped and dispersed in ethanol and casted on 300 mesh carbon-coated copper grid. The ITO is used as the back side ohmic contact to the diode. Schottky contacts to the front side of the polymer films were formed by vacuum evaporation at a base pressure of 5×10^{-6} Torr, using a shadow mask to form circular dots. Aluminum was chosen as the Schottky contact metal. The shadow mask used for the Schottky contacts was designed to produce an array of two devices on each sample, each with a dot diameter of approximately 4 mm.

Instruments

Bruker ultra shield 400 MHz NMR was used to obtain the proton NMR of the compounds. Q-Tof microTM Mass spectrometer was used to record the mass spectrum of the compound. Nicolet 5700 FTIR was used to identify the compounds and investigate sample composition in the wave number range of 4000–400 cm^{-1} with a resolution of 4 cm^{-1} . Small amount of the sample was mixed with KBr powder. A pellet of the mixture was prepared using a hydraulic press. Thermal analysis of the compounds was carried out by Mettler Toledo DSC822^e at heating and cooling rate of 10 °C/min in argon atmosphere at a flow rate of 80 mL/min. Q-Switched Nd-YAG (Nydodium-doped Yttrium Aluminum Garnet) laser source (Quanta ray INDI- Newport Corporation) was used as source for laser ablation. Thermo fisher scientific multilab 2000 X-ray photoelectron spectroscope was used to analyze the chemical composition of deposited films. Hydrodynamic radius and molecular weight of the polymer were characterized by using Viscotek 802 DLS equipment. Fragment size and distribution of polymer were characterized using Tecnai G-20 High Resolution TEM. Topographical characterization of the films was carried out by scanning electron microscopy using SEM-Sirion field emission. Thickness and surface roughness of the fabricated films were determined by Wyko NT1100 optical profilometer. Optical properties of the material were studied by T60 UV-visible spectrometer. Electrical conductivity was measured by Keithley 2182A (nanovoltmeter), 6221 (AC and DC sources). Current voltage (I – V) characteristics were carried out using Keithley 2612A dual source meter. Four probe head from Cascade Microtech with tungsten carbide tips

with radius of 0.5 μm and separated by 0.016 cm distance was used for the conductivity measurement.

Results and discussion

Thermogram of the polyDAD is shown in Fig. 2. Heating and cooling program were cycled thrice from 0 to 150 °C with a rate of 10 °C/min to identify reversible and non reversible transitions occurring in the polymer. To remove the thermal history and the effect of residual solvent, first heating cycle was not considered. In the second cycle, a melting endothermic peak around 104 °C with an enthalpy of melting of 7.74 J/g was observed which reappears at about the same temperature and enthalpy of melting on re-heating. This small reversible melting transition indicates that film morphology could be improved by annealing. These poly DAD films were found to be stable up to 300 °C (see supporting information Fig. 6).

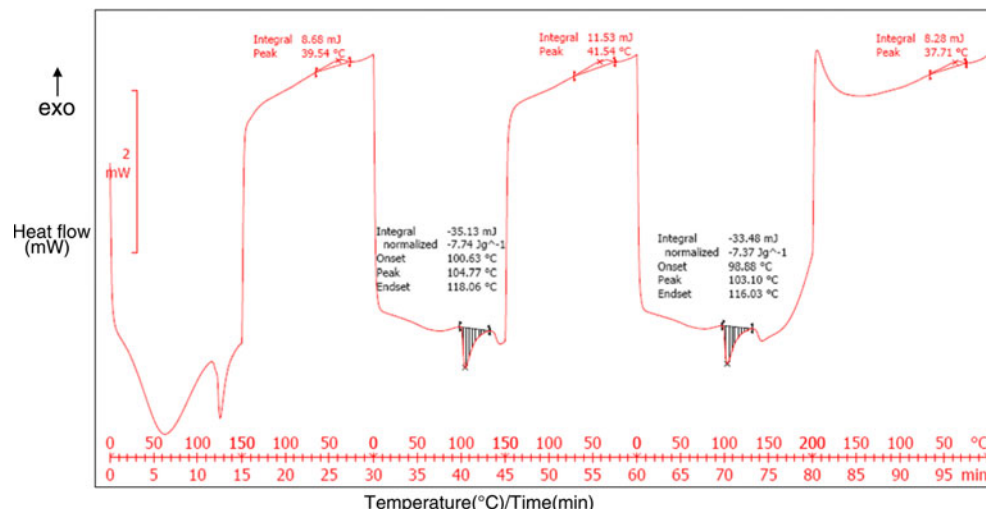
Chemical integrity of the films was characterized by X-ray photo electron spectroscopy. XPS spectra of as synthesized and ablated polyDAD are shown in Fig. 3. For the as synthesized, C1s peak is observed at 284.64 eV, it corresponds to C=C and C–H bonds. The peak at 286.13 eV indicates C=O. S2p peak at 164.3 eV indicates the thiophene group [26]. O1s peak is observed in the spectra at 532.2 eV. In case of film deposited by ablation, C1s peak is observed at 284.51 eV, which corresponds to C=C and C–H bonds. Peak at 285.82 eV corresponds to C=O and S2p peak at 164.1 eV indicates thiophene group. O1s peak is observed at 532.14 eV. Spectrum of both film deposited by ablation and as synthesized matches indicates that polyDAD material does not decompose during PLD. In addition, chemical integrity of the ablated films was evaluated by FTIR as shown in Fig. 4. The spectra of ablated films show all the peaks corresponding to the

functional groups observed in the neat polyDAD. Due to absorbed moisture in the ablated film, a peak around 3700 cm^{-1} was observed. FTIR and XPS data indicate that the chemical composition of polyDAD remains intact during ablation though the molecular weight may reduce [27].

Dynamic light scattering experiment was carried out for as synthesized and ablated polyDAD. Hydrodynamic radius and molecular weight of the polyDAD were determined from the experiment. Histogram of fragment size of as synthesized and ablated polyDAD is shown in Fig. 5. Hydrodynamic radii were found to be in the range of 43.2 (98.6% molecules) and 123.2 nm (1.4% molecules) with 1429.7 and 9686.5 kD molecular weight, respectively, for as synthesized polyDAD. The hydrodynamic radius and molecular weight decrease significantly for ablated material. It was found to be 17.01 nm and 269.77 kD, respectively. Here, almost 100% molecules has same hydrodynamic radius. During ablation, the polymer chain breaks, and smaller fragments with almost same hydrodynamic radius are ablated and deposited on the target. Since the size of the fragments deposited is same, the obtained film will be well packed. Hence the uniformity and smoothness of the ablated polyDAD film increases.

In addition to compare deposition characteristics of DAD and polyDAD, TEM analysis of the ablated materials were carried out. TEM images and fragment size distribution of ablated polyDAD and DAD films are shown in Figs. 6 and 7, respectively. The average fragment size distribution for polyDAD and DAD was found to be 17.3 nm and 4.6 μm , respectively. These TEM images reflect the fact that smaller fragments for polyDAD and comparatively bigger fragments for DAD were ablated. Consequently, polyDAD-ablated film appears to be compact, smoother, and continuous than the ablated DAD film. DLS results also show that the hydrodynamic radius is around 17 nm for ablated polyDAD.

Fig. 2 Differential scanning calorimetry thermogram of as synthesized polyDAD



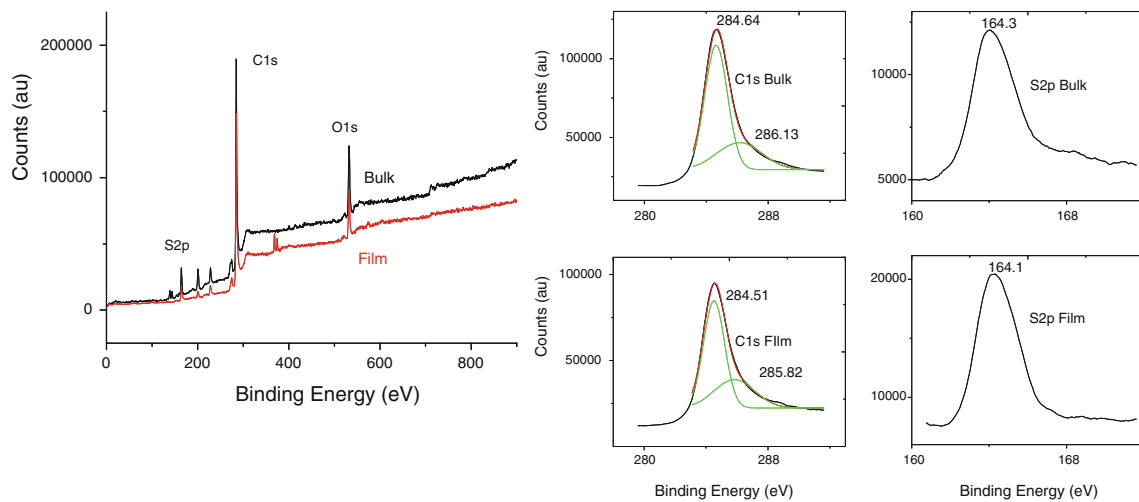


Fig. 3 X-ray photoelectron spectra of polyDAD as synthesized and ablated film

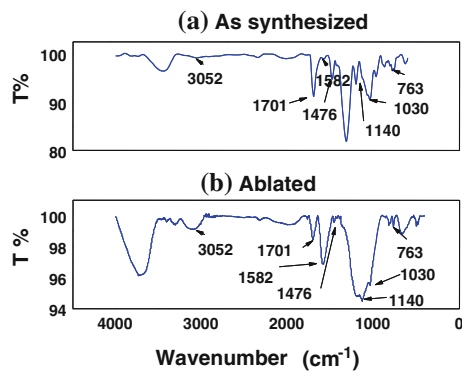


Fig. 4 The Fourier transform infrared (FTIR) spectra of as synthesized and ablated film polyDAD

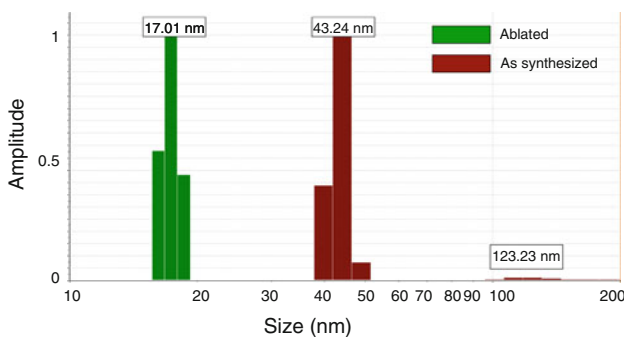


Fig. 5 Histogram of fragment size of as synthesized and ablated polyDAD

SEM images of DAD and polyDAD films are shown in Fig. 8. SEM image of polyDAD indicates that the film is smoother with speckled texture. During ablation, poly DAD small fragments of the polymer are ablated rather than bigger fragments as seen in DAD films. Consequently, the obtained film from polyDAD was more compact and continuous. SEM image of DAD shows that the film

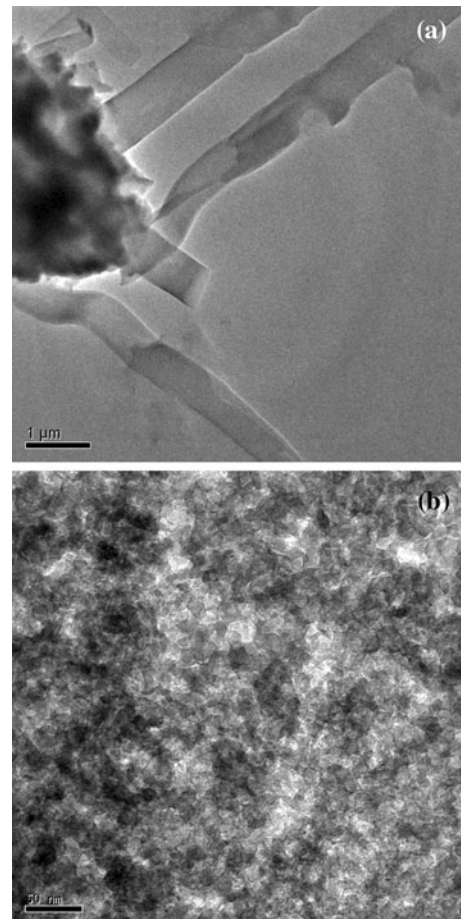


Fig. 6 Transmission electron micrographs of ablated **a** DAD and **b** polyDAD

appears to be made of bigger chunks of DAD. Hence DAD films found to be not continuous, but aggregation of bigger fragments. Roughness and thickness of the fabricated films on silicon wafer were determined by optical profilometry

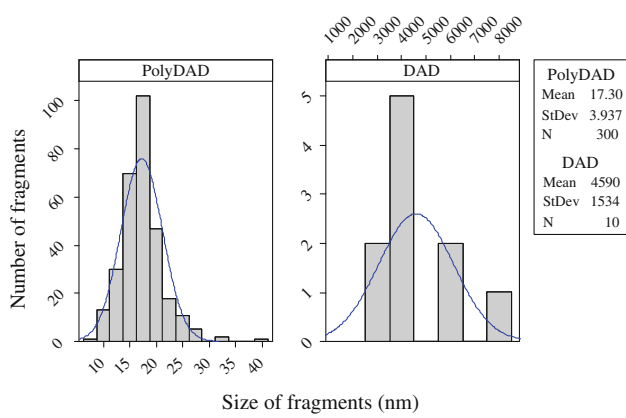


Fig. 7 Ablated fragment size distribution in films of DAD and polyDAD

(Fig. 9). Thickness and roughness of polyDAD film were found to be $0.450 \pm 0.02 \mu\text{m}$ and 76 nm, respectively. Thickness and roughness of DAD film were found to be 6.6 ± 0.13 and $5.9 \mu\text{m}$, respectively (Table 1).

Band gap and absorption ranges of the synthesized materials were determined by UV-visible spectroscopy. Absorption measurements were carried out in wavelength range 300–900 nm (Fig. 10). Band gap of both DAD and

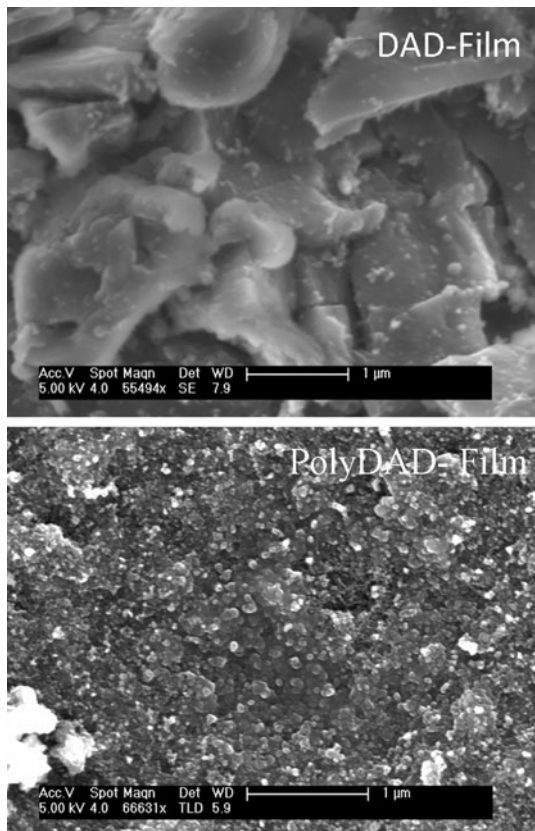


Fig. 8 Scanning electron micrographs of DAD and polyDAD ablated films

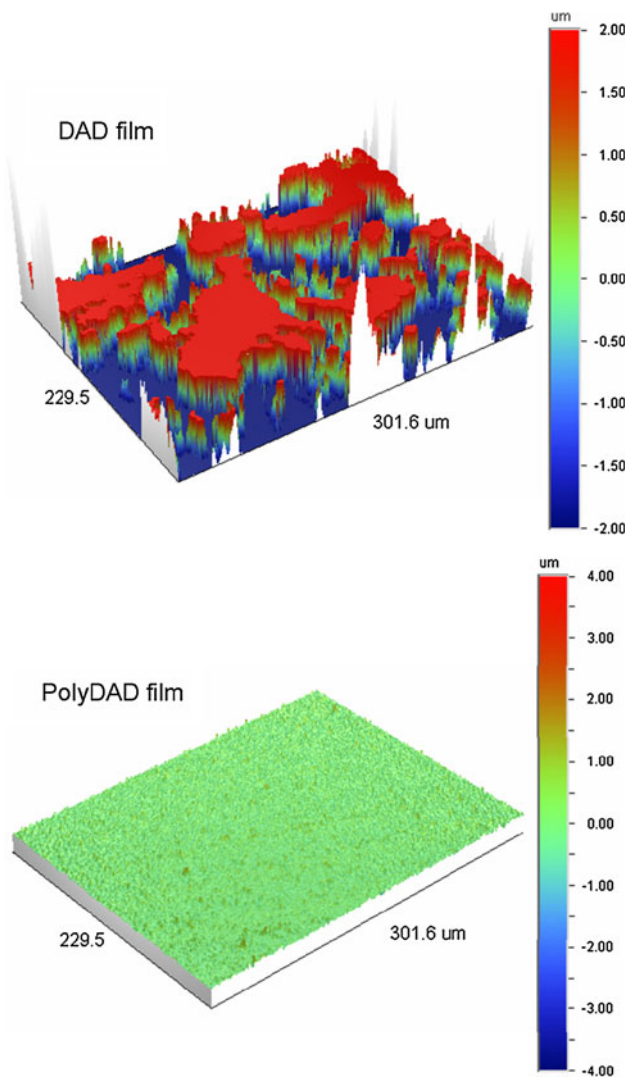


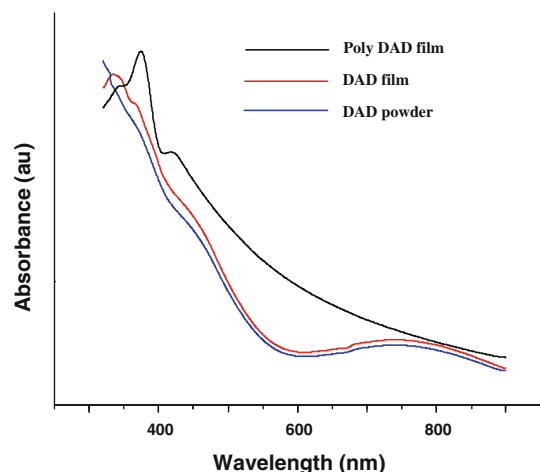
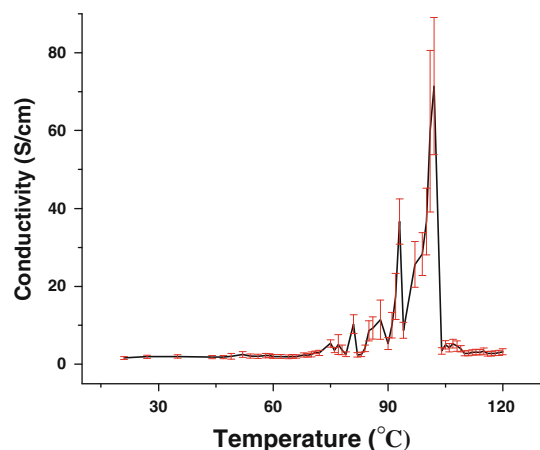
Fig. 9 Optical profilometer 3D images of ablated DAD and polyDAD film

polyDAD films deposited on glass substrates were determined from the wavelength corresponding to the absorption onset of 834 and 857 nm for DAD and polyDAD, respectively. The optical band gap was found to be 1.49 and 1.45 eV for the monomer and the polymer, respectively (Table 1). Walker et al. reported the band gap calculation of DAD and polyDAD material [17]. The peaks between 350 and 450 nm are due to the absorption of the glass substrate. Since polyDAD is insoluble in any of the organic solvents, previously it was not possible to experimentally determine band gap of polyDAD by optical measurements. Since thin films of the polymer were fabricated by PLD technique, band gap measurements could be carried out.

Conductivity of the as synthesized and pulsed laser deposited films of polyDAD and DAD were measured using four point probe set up. For the current range of

Table 1 Comparison of properties of DAD and polyDAD

	Bulk (S/cm)	Laser ablated film (S/cm)	Band gap (eV)	Roughness (RMS)	Thickness (μm)
DAD	$3.46 \times 10^{-4} \pm 0.0002$	$5.2 \times 10^{-4} \pm 0.00028$	1.49	6 μm	6 ± 0.13
Poly DAD	$8.09 \times 10^{-3} \pm 0.000073$	$4.62 \times 10^1 \pm 0.005$	1.45	70 nm	0.45 ± 0.02

**Fig. 10** UV-visible absorption spectra of DAD (as synthesized and film) and polyDAD film**Fig. 11** Temperature dependence of conductivity for ablated poly-DAD film

50–80 mA drop in voltage was measured, and conductivity was calculated using the equation. $\rho = \frac{\pi}{\ln 2} \times t \times \frac{V}{I}$, where t is the thickness of the film, V is the voltage, and I is the current. Average conductivity of the as synthesized DAD and polyDAD are measured to be 3.46×10^{-4} S/cm and 8.09×10^{-3} S/cm, respectively. Ablated polyDAD film shows an average conductivity of 4.62×10^1 S/cm and that of DAD is 5.2×10^{-4} S/cm (Table 1). In case of as synthesized, an order increase in conductivity was observed from DAD to polyDAD. Ablated films of

polyDAD show a remarkable increase in conductivity. Four orders of increase in conductivity were observed in ablated polyDAD film. These results indicate device quality film of polyDAD can be fabricated by PLD.

Conductivity of polyDAD film at various temperatures was measured (Fig. 11). Maximum conductivity was observed at about 104 °C and then conductivity decreases drastically. DSC data show that there is an endotherm around 104 °C indicating phase change. Hence this increase in conductivity can be attributed to phase change around this temperature. Furthermore, polyDAD film was annealed at 104 °C, and conductivity was measured. It was found that conductivity of annealed sample increased indicating increased ordering of the molecules upon heating.

I–*V* characteristics for the polyDAD films were measured and are as shown in Fig. 12. The schematic representation of the architecture of the device is as shown in supporting information (Fig. 7). These measured *I*–*V* curves exhibit nonlinear *I*–*V* characteristics, similar to that of a diode with a small rectification of about 3. A linear region on semi log *I*–*V* curve which is indicative of thermionic emission is observed as shown in the inset in Fig. 12. Due to the slight rectification, the Schottky parameters were extracted [28, 29]. According to thermionic emission model, relation between current and voltage is given as

$$J = J_0 \exp\left(\frac{qV}{\eta kT}\right)$$

where J_0 is the saturation current density, q is electronic charge, η is ideality factor, k is Boltzmann constant, and T is absolute temperature. Barrier height ϕ_b can be calculated from the Richardson equation for thermionic emission.

$$J_0 = A^* T^2 \exp\left(\frac{-q\phi_b}{kT}\right)$$

where A^* is the Richardson constant taken as 120 for most p-type conducting polymers. Ideality factor and barrier height were calculated from the linear fit for the semi log plot of *I*–*V* (inset Fig. 12). Ideality factor was found to be 23 and barrier height calculated was 0.67 eV. The high value of ideality factor in the case of polymer diodes has been attributed to metal semiconductor interfacial roughness, in addition to the inherent resistance and low mobility. In addition, photovoltaic characteristics of these devices are being evaluated.

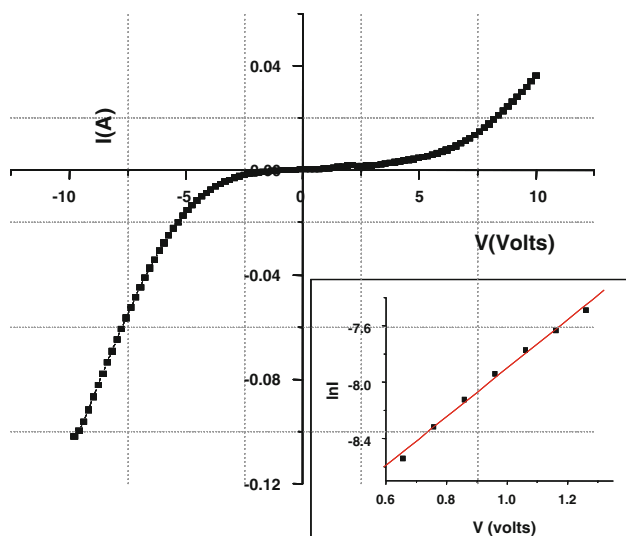


Fig. 12 I - V characteristics of the Schottky device (semi log plot of I - V is shown in the inset)

Conclusions

PolyDAD was synthesized from DAD monomer because it offers a better architecture for exciton dissociation and charge transportation in case of a photovoltaic device. PolyDAD neither soluble in any solvent, nor it can be melt processable, hence device quality films can not be fabricated by techniques like spin coating, melt forming etc. Consequently, PLD technique was employed for fabrication of device quality film. XPS and FTIR data of both as synthesized and ablated film match well which indicates the material does not degrade during ablation. DLS analysis shows that there is a reduction in hydrodynamic radius and molecular weight in the ablated polyDAD. TEM analysis of polyDAD film indicates that the film is compact and continuous due to the ablation of smaller and uniform fragments. UV Visible absorption of DAD and polyDAD ranges from 300 to 900 nm, and optical band gap was determined to be 1.49 and 1.45 eV, respectively. Conductivity of DAD was found to increase by an order of magnitude when polymerized. Increased conductivity observed from DAD to polyDAD in case of as synthesized was further increased by four orders of magnitude after fabrication of film by PLD. Conductivity study with temperature shows that it is possible to increase conductivity of polyDAD film by annealing. Schottky devices fabricated without optimizing the architectures indicate the scope for further improvement in the device quality. These results indicate that PLD is a suitable technique for fabrication of device quality film of polymers. Further optimization of photovoltaic device fabrication and characterizations are currently underway.

Acknowledgements This study is partially supported by KRCF (Korea Research Council of Fundamental Science & Technology) and KIST (Korea Institute of Science & Technology) for 'NAP (National Agenda Project) program. In addition, authors gratefully acknowledge the financial support from DST No SR/S3/ME/025/2008, technical support from IISc advanced characterization center, Prof K. Chatopadhyay's laser lab and NMR research centre.

References

- Young Z, Stevan KH, Hin-Lap Y, Ying S, Orb A, Alex KYJ (2010) Chem. Mater 22:2696
- Brabec CJ, Sariciftci NS, Hummelen JC (2001) Adv Funct Mater 11:15
- Brabec CJ (2004) Sol Energy Mater Sol Cells 83:273
- Peumans P, Yakimov A, Forrest SR (2003) J Appl Phys 93:3693
- Zhou Y, Peng P, Han L, Tian W (2007) Synth Met 157:502
- Koeppen R, Bossart O, Calzaferri G, Sariciftci NS (2007) Sol Energy Mater Sol Cells 91:986
- Steckler TT, Zhang X, Hwang J, Honeyager R, Ohira S (2009) J Am Chem Soc 131:2824
- Park SH, Roy A, Beaupre S, Cho S, Coates N, Moses JSMD, Leclerc M, Lee K, Heeger AJ (2009) Nat Photon 3:297
- Masuda K, Ogawa M, Ohkita H, Benten H, Ito S (2009) Sol Energy Mater Sol Cells 93:762
- Reyes MR, Lopez-Sandoval R, Liu J, Carroll DL (2007) Sol Energy Mater Sol Cells 91:1478
- Spanggaard H, Krebs FC (2004) Sol Energy Mater Sol Cells 83:125
- Gunes S, Neugebauer H, Sariciftci NS (2007) Chem Rev 107:1324
- Rand BP, Genoe J, Heremans P, Poortmans J (2007) Prog Photovolt Res Appl 15:659
- Bundgaard E, Krebs FC (2007) Sol Energy Mater Sol Cells 91:954
- Berlin A, Brenna E, Pagani GA, Sannicolb F (1992) Synth Met 5:287
- Kraak A, Wersema AK, Jordens P, Wynberg H (1968) Tetrahedron 24:3381
- Walker W, Veldman B, Chiechi R, Patil S, Bendikov M (2008) Macromolecules 41:7278
- Zotti G, Schiavon G (1994) Macromolecules 27:1938
- Lodha A, Kilbey SM, Ramamurthy PC, Gregory RVJ (2001) Appl Polym Sci 82:3602
- Siew WO, Tou TY, Wong KH (2005) Appl Surf Sci 248:281
- Kim KC, Park JH, Park OO (2008) Sol Energy Mater Sol Cells 92:1188
- Cossement D, Plumier F, Delhalle J, Hevesi L, Mekhalif Z (2003) Synth Met 138:529
- Ferguson JD, Arikan G, Dale DS, Woll AR, Brock JD (2009) Phys Rev Lett 103:256103
- Ohnishi T, Shibuya K, Yamamoto T, Lippmaa M (2008) J Appl Phys 103:103703
- Lim H, Choi JH (2006) J Chem Phys 124:14710
- Lachkar A, Selmani A, Sacher E, Leclerc M, Mokhliss R (1994) Synth Met 66:209
- Nishio S, Chiba T, Matsuzaki A (1996) J Appl Phys 79:7198
- Sze SM (1981) Physics of semiconductor devices. Wiley, New York
- Ramamurthy PC, Malshe AM, Harrell WR, Gregory RV, McGuire K, Rao AM (2003) Mater Res Soc Symp Proc 772:M4.3.1